Journal of Elasticity
https://doi.org/10.1007/s10659-022-09972-7

Options for Dynamic Similarity of Interacting Fluids, Elastic Solids and Rigid Bodies Undergoing Large Motions

Huan Liu[1] · Kalpesh Jaykar[1] · Vinitendra Singh[1] · Ankit Kumar[1] · Kevin Sheehan[1] · Peter Yip[1] · Philip Buskohl[2] · Richard D. James[1]

Received: 31 October 2022 / Accepted: 12 December 2022
© The Author(s), under exclusive licence to Springer Nature B.V. 2023

Abstract
Motivated by a design of a vertical axis wind turbine, we present a theory of dynamical similarity for mechanical systems consisting of interacting elastic solids, rigid bodies and incompressible fluids. Throughout, we focus on the geometrically nonlinear case. We approach the analysis by analyzing the equations of motion: we ask that a change of variables take these equations and mutual boundary conditions to themselves, while allowing a rescaling of space and time. While the disparity between the Eulerian and Lagrangian descriptions might seem to limit the possibilities, we find numerous cases that apparently have not been identified, especially for stiff nonlinear elastic materials (defined below). The results appear to be particularly adapted to structures made with origami design methods, where the tiles are allowed to deform isometrically. We collect the results in tables and discuss some particular numerical examples.

Keywords Dynamic similarity · Scaling laws · Fluid-structure interaction · Wind turbines · Material selection · Continuum mechanics

Mathematics Subject Classification Primary 70G65 · 74F10 · Secondary 70E99 · 74B20 · 76D99

1 Introduction

A powerful tool in fluid and solid dynamics is dynamic similarity. In this paper we consider its use in the design of structures involving parts that are highly deformable, together with components that are nearly rigid, immersed in a complex fluid flow that may be unsteady and turbulent. Structures having these features are encountered increasingly for the mitigation of climate change by emerging concepts for the generation of power from wind and flowing water; this is the context in which the need for a theory arose for the authors

✉ R.D. James

[1] Department of Aerospace Engineering and Mechanics, University of Minnesota, Minneapolis, MN 55455, USA

[2] Materials and Manufacturing Directorate, Air Force Research Laboratory, Wright-Patterson AFB, Dayton, OH 45433, USA

Published online: 12 January 2023

Fig. 1 Example of a structure of the type considered here. The blades are deformable (see Fig. 2) and could reasonably be treated by geometrically nonlinear elasticity, the central rotator and supports are naturally modeled as rigid bodies and the surrounding air as a Navier-Stokes fluid

(Fig. 1). In such cases the existence or reliability of numerical methods is in question and validation of such methods by, say, wind/water tunnel testing is in any case desirable. Often these structures also contain rotating parts, which further necessitates the use of geometrically nonlinear theory. In addition, examples of this type often include thin structures, rigid bodies or disconnected deformable bodies. Our results apply in that case, but we only show connected bodies of each type in Fig. 1.

Dynamic similarity is an ancient subject. Surely, Archimedes, in his studies of the floating of simple objects such as paraboloids of revolution, knew that the behavior of one such object implied the behavior of all such objects [1]. Euler's precise treatment of beams [2] and the stability of ships [3–5] contained explicit combinations of material and geometric constants suitable for dynamic similarity.

A treatment of the modern view of dynamic similarity (termed similitude) from an engineering perspective is presented by Coutinho et al. [6], Kline [7], and Casaburo et al. [8]. They distinguish the use of classical dimensional analysis from the use of differential equations to establish similitude. In the former case there is an algebraic relation between the quantities of interest, and this is usually exploited by using the Buckingham π theorem ([9]. A natural application of this method is to the simplification of a proposed constitutive relation (Examples given in [10]).

The use of differential equations relies in a more general way on the fundamental law that all equations of physics are invariant under a change of units, whether differential, algebraic or more general. With differential equations the usual procedure is to put the equations in a dimensionless form, and to identify various combinations of material constants that give rise to the same solution rescaled to a different domain and a different time scale.

From a mathematical viewpoint (where units are usually not mentioned), the equivalent procedure is to find a symmetry of the differential equation, i.e., a change of variables that transforms a solution to another solution. This is more general than the procedure of nondimensionalization. In other words, after nondimensionalizing the given equations, there may be additional symmetries. They are also candidates for the demonstration of dynamical similarity. An example to explain such a symmetry is the heat equation $u_t = u_{xx}$, where $u(x,t) = e^{-\epsilon x+\epsilon^2 t} f(x-2\epsilon t, t)$ solves the heat equation whenever $f(x,t)$ is a solution. See [11], where many other examples and their associated Lie groups are given.

In the case treated here of deformable bodies interacting with rigid bodies and incompressible fluids, which are themselves interacting with each other, we are unable to find a treatment in the generality considered here, and it is not clear at the outset that there is any opportunity for dynamic similarity. However, surprisingly, we find various possibilities, particularly in cases of stiff bodies where geometrically nonlinear/physically linear models apply.[1] Structures like this are ubiquitous in origami design [12–14]; the fact that they can be folded from a flat state is considered as an advantage with regard to transportation and deployment of the structure. In this case unusual scalings involving elastic moduli as well as space, time, viscosity, density, Lagrangian motions of the solids, Eulerian velocity of the fluid, and other geometric factors are possible.

The search for scaling laws forces us to say precisely how, for example, the fluid interacts with the elastic solid. Then we have to check that this interaction is consistent with the scaling laws we find. In the particular case of the elastic solid interacting with the fluid, we say that the fluid provides a traction boundary condition on the elastic solid. Conversely, we say that the elastic solid imposes a no-slip boundary condition on the fluid. Similar decisions are made for the other interactions. We based these decisions on physical considerations discussed in Sect. 7. From a mathematical viewpoint this issue concerns the well-posedness of the full coupled system of equations, and almost nothing is known about this.[2] We summarize the full system of equations and boundary conditions for which the final scaling laws hold in Sect. 7. We hope that these physical considerations can guide future work on well posedness in this area. In general in this paper we suppress smoothness assumptions.

For quick reference we summarize all the cases of dynamical similarity that we find in Sect. 6. To further highlight the usefulness of the results we give some numerical examples.

2 Basic Set-up, Kinematics and Notation

We consider three types of bodies: a general nonlinear elastic solid, a rigid body and an incompressible Navier-Stokes fluid. We do not consider body forces.[3] We allow mutual interactions between all pairs of these bodies. Fig. 1 shows a schematic. Our results also apply in complex cases, for example, there are several disconnected rigid bodies or disconnected deformable bodies.

In all cases we scale the solid structures uniformly in space as shown in Fig. 2. We use the Lagrangian form of the equations for solid structures. Therefore, both the elastic solid and rigid body have reference configurations labelled, respectively, Ω and Ω_r. This is to take advantage of "elasticity scaling", which also applies exactly to the Lagrangian form of the equations of rigid body mechanics. These reference configurations meet at $\mathcal{S} = \partial\Omega \cap \partial\Omega_r$.

We use the suggestive terminology *laboratory model* and *full-scale model* to describe reference and deformed configurations in both cases. The laboratory model can be made of different materials than the full-scale model, and the fluid in the laboratory model can have

[1] We emphasize that in this paper the deformable body is allowed to undergo large motions. Thus, the linearizations that are common in problems of fluid-structure interaction and particularly in aerodynamics are not considered here.

[2] The conditions for well-posedness of the dynamic nonlinear elastic system by itself are not known in the general case; the state of knowledge is presented by [15]. The well-posedness of the system of equations for the rigid body is trivial, see below.

[3] All equations are written in the common inertial frame fixed to the laboratory and full-scale models, so centrifugal forces are accounted for in our geometrically nonlinear treatment. Often, steady centrifugal forces are treated as a body force in a rotating frame. Here, centrifugal forces are accounted for even if they are unsteady and, for example, cause unwanted vibrations.

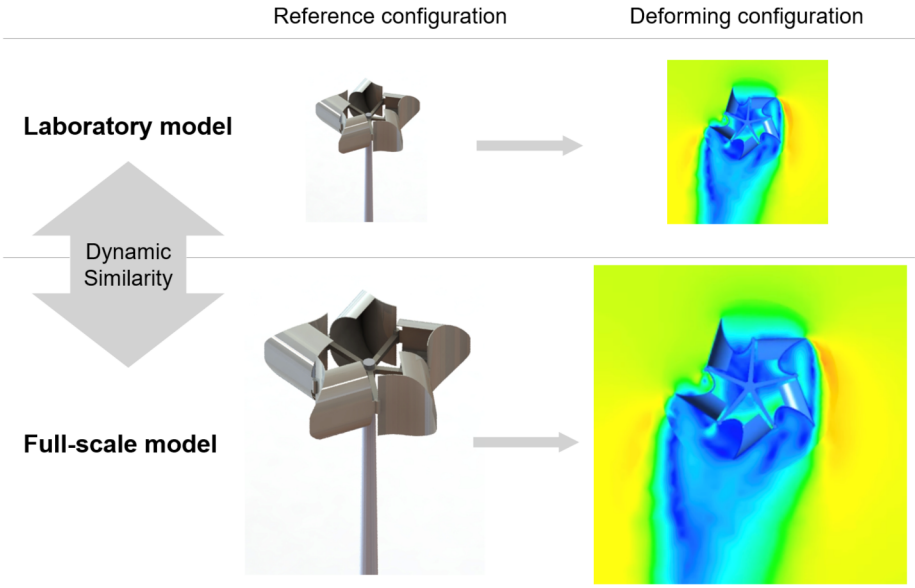

Fig. 2 An example to show the laboratory model and the full-scale model, where the reference configuration of a VAWT and its deforming configuration (top view) are scaled. Note the asymmetry of the fluid flow arising from the shape and deformability of the blades in this origami design

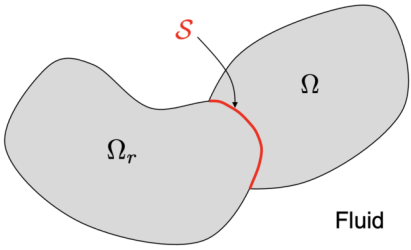

Fig. 3 Schematic of the elastic solid Ω, the rigid body Ω_r and their interface $\mathcal{S}$. The fluid domain is $\mathbb{R}^3 \setminus \Omega \cup \Omega_r$

different viscosity, density and pressure than the full-scale model. The rigid body can be inhomogeneous. The elastic body is also allowed to be inhomogeneous but the scaling laws place restrictions on the inhomogeneity.

The motion of the elastic body is denoted by $\mathbf{y}(\mathbf{x}, t),\ \mathbf{x} \in \Omega$ and the motion of the rigid body is $\mathbf{y}_r(\mathbf{x}, t),\ \mathbf{x} \in \Omega_r$. Ω and Ω_r are fixed reference configurations and $\mathbf{x}$ is a material coordinate throughout. The motion of the fluid is described by an Eulerian velocity field $\mathbf{v}(\mathbf{y}, t),\ \mathbf{y} \in \mathbb{R}^3 \setminus \big(\mathbf{y}(\Omega, t) \cup \mathbf{y}_r(\Omega_r, t)\big)$ (see Fig. 3). Thus, we use the letter $\mathbf{y}$ as both an independent and a dependent variable. Where this notation could cause confusion, we replace the independent variable $\mathbf{y}$ by $\mathbf{r}$. To describe the interaction of solid bodies on the fluid, we will have to find the Eulerian velocity field of solid bodies. We will convert the velocities by using the standard relation between Eulerian (E) and Lagrangian (L) descriptions, e.g.,

$$\begin{aligned} E \longrightarrow L: &\ \text{Solve the infinite system of ODEs: } \dot{\mathbf{y}}(\mathbf{x}, t) = \mathbf{v}(\mathbf{y}(\mathbf{x}, t), t),\ \ \mathbf{y}(\mathbf{x}, 0) = \mathbf{x},\ \ \mathbf{x} \in \Omega, \\ L \longrightarrow E: &\ \text{Invert and evaluate: } \mathbf{v}(\mathbf{y}, t) = \dot{\mathbf{y}}(\mathbf{y}^{-1}(\mathbf{y}, t), t),\ \ \mathbf{y} \in \mathbb{R}^3 \setminus \big(\mathbf{y}(\Omega, t) \cup \mathbf{y}_r(\Omega_r, t)\big). \end{aligned} \tag{1}$$

A superimposed dot represents the time derivative of a function of $(\mathbf{x}, t)$.

The most convenient form for the kinematics of the rigid body is as follows. Ω_r is given and we also assume that the reference density $\rho_r(\mathbf{x})$, $\mathbf{x} \in \Omega_r$, is given for the laboratory model. The general form of the motion of a rigid body can be written as

$$\mathbf{y}_r(\mathbf{x}, t) = \mathbf{R}(t)(\mathbf{x} - \mathbf{x}_{cm}) + \mathbf{y}_{cm}(t), \quad t > 0, \ \mathbf{x} \in \Omega_r, \tag{2}$$

where $\mathbf{R}(t) \in \mathrm{SO}(3)$ and $\mathbf{x}_{cm}$ denotes the center of mass in the reference configuration, which is

$$\mathbf{x}_{cm} = \frac{1}{M_r}\int_{\Omega_r} \rho_r(\mathbf{x})\mathbf{x}\, d\mathbf{x}, \quad \mathbf{y}_{cm}(t) = \frac{1}{M_r}\int_{\mathbf{y}_r(\Omega_r)} \rho_r(\mathbf{y}_r^{-1}(\mathbf{r}, t))\mathbf{r}\, d\mathbf{r}, \quad M_r = \int_{\Omega_r} \rho_r(\mathbf{x})\, d\mathbf{x}. \tag{3}$$

Here SO(3) denotes the set of rotation tensors in 3 dimensions (in an orthonormal basis, 3×3 rotation matrices), $\mathrm{SO}(3) = \{\mathbf{R} : \mathbf{R}^T\mathbf{R} = \mathbf{I}, \ \det\mathbf{R} = 1\}$. The function $\mathbf{y}_{cm}(t)$ has the interpretation as the center of mass in the deformed configuration of the rigid body at time t. We use the following fact below: let a skew tensor $\mathbf{W}(t) = -\mathbf{W}^T(t)$, $t > 0$ be given, and solve the system of ordinary differential equations $\dot{\mathbf{Q}}(t) = \mathbf{Q}(t)\mathbf{W}(t)$, subject to the initial conditions $\mathbf{Q}(0) = \mathbf{Q}_0$. A general fact is that, if $\mathbf{Q}_0 \in \mathrm{SO}(3)$, then $\mathbf{Q}(t) \in \mathrm{SO}(3)$ for $t > 0$. We shall also need the inertia tensor for the reference configuration of the rigid body, defined by

$$\mathcal{I} = \int_{\Omega_r} \rho_0(\mathbf{x})\big[|\mathbf{x} - \mathbf{x}_{cm}|^2\mathbf{I} - (\mathbf{x} - \mathbf{x}_{cm}) \otimes (\mathbf{x} - \mathbf{x}_{cm})\big]d\mathbf{x}. \tag{4}$$

By the Cauchy-Schwarz inequality $\mathcal{I}$ is positive-definite.

3 Equations of Motion

We summarize the equations of motion for the three types of bodies, written for the laboratory model. The interaction conditions are treated in Sect. 4.

3.1 Rigid Body

Consider first the rigid body with reference domain Ω_r. It is assumed to be acted upon by a resultant force $\mathbf{f}(t)$ and moment $\mathbf{m}(t)$, $t > 0$, these being produced by the fluid and elastic solid. The equations of motion of the rigid body are:

$$\begin{aligned} M_r\ddot{\mathbf{y}}_{cm}(t) &= \mathbf{f}(t), \\ \mathcal{I}\dot{\mathbf{w}} &= -\mathbf{w} \times \mathcal{I}\mathbf{w} - \mathbf{R}(t)^T\big(\mathbf{y}_{cm}(t) \times \mathbf{f}(t)\big) + \mathbf{m}(t), \\ \dot{\mathbf{R}} &= \mathbf{R}\mathbf{W}, \quad \mathbf{w} = \mathrm{axl}(\mathbf{W}), \end{aligned} \tag{5}$$

where $\mathbf{W}$ is a skew tensor with axial vector $\mathbf{w}$. In rectangular Cartesian components, $W_{ik} = \varepsilon_{ijk}w_j$, where ε_{ijk} is the permutation symbol. The system of three equations (5) is a system of ordinary differential equations in standard form. Hence, given $\mathbf{f}(t)$ and $\mathbf{m}(t)$ these equations are solved for $\mathbf{y}_{cm}(t), \mathbf{w}(t), \mathbf{R}(t)$ subject to initial conditions $\mathbf{y}_{cm}(0) = \mathbf{y}_{cm}^0$, $\mathbf{w}(0) = \mathbf{w}^0$, $\mathbf{R}(0) = \mathbf{R}^0$ with $\mathbf{R}^0 \in \mathrm{SO}(3)$. By the remark at the end of Sect. 2, the solution $\mathbf{R}(t)$ is in SO(3). Since $\mathbf{x}_{cm}$ is given, a solution of (5) fully determines the motion (2) of the rigid body. The equations (5) can be found by substituting (2) into the standard Lagrangian form of the balances of linear and rotational momentum of continuum mechanics.

3.2 Elastic Solid

It is most convenient here to give the nonlinearly elastic solid in Lagrangian form. For that purpose we specify a constitutive relation for the Piola-Kirchhoff stress of the form $\mathbf{T}(\mathbf{F}, \mathbf{x})$, where $\mathbf{F} = \nabla \mathbf{y}$ is the deformation gradient. The explicit dependence on $\mathbf{x}$ represents inhomogeneity of the material; this allows us to consider composites. We assume $\mathbf{T}(\mathbf{F}, \mathbf{x})$ is defined for $\det \mathbf{F} > 0$ and $\mathbf{x} \in \Omega$ and satisfies the principle of material frame indifference $\mathbf{T}(\mathbf{QF}, \mathbf{x}) = \mathbf{QT}(\mathbf{F}, \mathbf{x})$ for all $\mathbf{Q} \in \mathrm{SO}(3)$, all $\mathbf{F}$ with $\det \mathbf{F} > 0$, and all $\mathbf{x} \in \Omega$. $\mathbf{T}$ is related to the familiar Cauchy stress by the formula $\boldsymbol{\sigma} = (1/\det \mathbf{F})\mathbf{T}\mathbf{F}^T$. Later, the explicit dependence of $\mathbf{T}$ on $\mathbf{x}$ will be further restricted to be consistent with scaling. The equations of motion of the elastic solid are

$$\rho_0(\mathbf{x})\ddot{\mathbf{y}} = \mathrm{div}_{\mathbf{x}}\mathbf{T}, \quad \mathbf{x} \in \Omega, \tag{6}$$

or, expanded and in rectangular Cartesian components,

$$\rho_0(\mathbf{x})\ddot{\mathbf{y}}_i(\mathbf{x}, t) = \frac{\partial T_{ij}(y_{p,q}(\mathbf{x}, t), \mathbf{x})}{\partial F_{k\ell}} y_{k,\ell j}(\mathbf{x}, t) + \frac{\partial T_{ij}(y_{p,q}(\mathbf{x}, t), \mathbf{x})}{\partial x_j}. \tag{7}$$

The equations of nonlinear elasticity place the strongest restriction on possible scaling laws, since they must be applicable to all materials, i.e., all functions $\mathbf{T}(\mathbf{F}, \mathbf{x})$ with perhaps a special dependence on $\mathbf{x}$. However, besides the standard "elasticity scaling" that we use below, we consider another interesting case that covers geometrically nonlinear elasticity theory for physically linear/ geometrically nonlinear elasticity. To explain this case, we assume that there is a stored energy function $\varphi(\mathbf{F}, \mathbf{x})$, which is a potential for the Piola-Kirchhoff stress: $\mathbf{T} = \partial\varphi/\partial\mathbf{F}$. This assumption is justified by thermodynamic arguments [16]. In addition, it is usually assumed that $\varphi(\mathbf{F}, \mathbf{x}) \geq \varphi(\mathbf{I}, \mathbf{x})$. Together with frame-indifference, this implies that φ is minimized on SO(3). If for some reason (thinness, or the stresses are small) the deformation gradient remains mainly near SO(3) in a suitable sense, then the response of the material is governed by the linear elastic moduli.

The typical way to formulate an explicit model of this type is to replace the geometrically linear strain measure by a nonlinear strain measure in the stress-strain law of linear elasticity. The classic example for an isotropic material is due to St. Venant and Kirchhoff (see [10], p. 348), based on the relation

$$\tilde{\mathbf{T}} = \lambda(\mathrm{tr}\mathbf{E})\mathbf{I} + 2\mu\mathbf{E}, \tag{8}$$

where $\mathbf{E} = \frac{1}{2}(\mathbf{F}^T\mathbf{F} - \mathbf{I})$ is the Green strain, $\tilde{\mathbf{T}}$ is the second Piola-Kirchhoff stress and λ, μ are the Lamé moduli. The corresponding (first) Piola-Kirchhoff stress is

$$\mathbf{T}(\mathbf{F}, \mathbf{x}) = \frac{E(\mathbf{x})}{2}\left(\frac{\hat{\nu}(\mathbf{x})}{(1+\hat{\nu}(\mathbf{x}))(1-2\hat{\nu}(\mathbf{x}))}\left(\mathrm{tr}(\mathbf{F}^T\mathbf{F}) - 3\right)\mathbf{I} + \frac{1}{1+\hat{\nu}(\mathbf{x})}\left(\mathbf{F}\mathbf{F}^T - \mathbf{I}\right)\right)\mathbf{F}, \tag{9}$$

where we have traded Young's modulus E and Poisson's ratio $\hat{\nu}$ for the Lamé moduli.[4] The corresponding free energy is given in [17].

In fact, the St. Venant-Kirchhoff model has a defect: it fails the condition of rank-1 convexity at certain states of strong compression, see also [17]. Essentially, stiff materials or sufficiently thin bodies primarily see deformation gradients near SO(3), but the particular relation (9) should generally not be used for soft materials in compression.

[4] The hat on ν distinguishes it from the kinematic viscosity introduced below.

The St. Venant-Kirchhoff and related models are widely used and quite reasonable for stiff materials. They gain flexibility for the scaling, because the linear elastic moduli can be part of the scaling while the theory remains fully geometrically nonlinear. That is, the elastic material of the laboratory model can be made different from that of the full-scale model as long as it is tuned appropriately. Moreover, $\mathbf{T}(\mathbf{F}, \mathbf{x})$ in (9) is linear in Young's modulus $E(\mathbf{x})$. From the viewpoint of material selection one can find lots of materials with nearly the same value of Poisson's ratio ($\approx 1/3$) but highly tunable values of Young's modulus. Thus, below, we will consider the scaling of Young's modulus. We want to emphasize that the terminology "stiff" refers to a large Young's modulus. Large deformations with large rotations are still allowed.

Relatedly, rigorous derivations of nonlinear plate theory from a general version of 3D nonlinear elasticity are consistent with the exact use of constitutive equations that replace the small strain tensor by a corresponding finite strain tensor in the linearized theory. This situation occurs in the Kirchhoff energy of nonlinear plate theory [18], where the free energy is proportional to a single plate modulus, $2\mu + \frac{\lambda\mu}{\mu+\lambda/2}$. However, the passage from the plate theory to a geometrically nonlinear Piola-Kirchhoff stress in the manner of the St. Venant-Kirchhoff model is unclear, though we believe that this should be possible. More general models for anisotropic materials can also be used, but the selection of materials becomes more difficult.

3.3 Incompressible Navier-Stokes Fluid

The motion of the fluid is characterized by an Eulerian velocity field $\mathbf{v}(\mathbf{y}, t)$ and pressure field $p(\mathbf{y}, t)$ defined on the domain exterior to the rigid and elastic bodies. The equations of motion are

$$\mathbf{v}_t + \nabla\mathbf{v}\,\mathbf{v} = -\nabla p + \nu\Delta\mathbf{v}, \quad \operatorname{div}\mathbf{v} = 0, \quad \mathbf{y} \in \mathbb{R}^3 \setminus \big(\mathbf{y}(\Omega, t) \cup \mathbf{y}_r(\Omega_r, t)\big), \quad t > 0, \tag{10}$$

to be solved for $\mathbf{v}(\mathbf{y}, t)$ and $p(\mathbf{y}, t)$ (pressure/density). The material constant ν is the kinematic viscosity (viscosity/density). The density of the fluid is $\rho_f = const.$ and Cauchy stress in the fluid is

$$\boldsymbol{\sigma} = \rho_f\big(-p\mathbf{I} + \nu(\nabla\mathbf{v} + \nabla\mathbf{v}^T)\big). \tag{11}$$

4 Interaction Conditions

Any rescaling must preserve the interactions (i.e., mutual boundary conditions) between bodies, so that they are satisfied for the full-scale model if and only if they are satisfied for the laboratory model. As explained in the introduction, in the absence of a theorem of well-posedness, there is arbitrariness in the specification of interaction conditions, and we are guided here by what is known about special cases.

We have three kinds of interactions, elastic-rigid, elastic-fluid and rigid-fluid. The rigid body is special in two ways: it requires a specification of a resultant force $\mathbf{f}(t)$ and resultant moment $\mathbf{m}(t)$, and it is governed by ordinary differential equations. We assume that the force and moment on the rigid body are contributed by the elastic solid and the fluid:

$$\mathbf{f}(t) = \int_{\mathcal{S}} \mathbf{T}(\nabla\mathbf{y}(\mathbf{x}, t), \mathbf{x})\mathbf{n}_0\, da_0 + \int_{\mathbf{y}(\partial\Omega_r \setminus \mathcal{S})} \boldsymbol{\sigma}(\mathbf{r}, t)\mathbf{n}\, da,$$

$$\mathbf{m}(t) = \int_{\mathcal{S}} \mathbf{y}(\mathbf{x},t) \times \mathbf{T}(\nabla \mathbf{y}(\mathbf{x},t),\mathbf{x})\mathbf{n}_0\, da_0 + \int_{\mathbf{y}(\partial\Omega_r \setminus \mathcal{S})} \mathbf{r} \times \boldsymbol{\sigma}(\mathbf{r},t)\mathbf{n}\, da. \tag{12}$$

Here $\mathbf{n}_0$ is the outward unit normal to $\mathcal{S} \subset \partial\Omega_r$ and $\mathbf{n}$ is the outward unit normal to $\mathbf{y}(\partial\Omega_r \setminus \mathcal{S})$.

Conversely, the rigid body imposes forces on the elastic body and fluid. These forces cannot be calculated directly because the stress in a rigid body is arbitrary. However, the detailed motion is specified. Thus, we assume that the rigid body imposes a kinematic condition on the fluid in the form of a no-slip condition:

$$\begin{aligned}\mathbf{v}(\mathbf{r},t) &= \dot{\mathbf{y}}_r\left(\mathbf{y}_r^{-1}(\mathbf{r},t),t\right)\\ &= \dot{\mathbf{R}}\mathbf{R}^T(\mathbf{r} - \mathbf{y}_{cm}(t)) + \dot{\mathbf{y}}_{cm}(t), \quad \mathbf{r} \in \mathbf{y}_r(\partial\Omega_r \setminus \mathcal{S},t),\ t > 0.\end{aligned} \tag{13}$$

For the same reason we assume that the rigid body imposes displacement conditions on the elastic body:

$$\mathbf{y}(\mathbf{x},t) = \mathbf{y}_r(\mathbf{x},t), \quad \mathbf{x} \in \mathcal{S},\ t > 0. \tag{14}$$

The conditions (13) and (14) can each be thought of as "half boundary conditions", the other half being represented by (12). Similarly, we expect that there are two additional boundary conditions for the fluid and elastic body. We think that the most reasonable choices from a physical viewpoint is a no-slip boundary condition for the fluid imposed by the elastic solid,

$$\mathbf{v}(\mathbf{r},t) = \dot{\mathbf{y}}\left(\mathbf{y}^{-1}(\mathbf{r},t),t\right), \quad \mathbf{r} \in \mathbf{y}(\partial\Omega \setminus \mathcal{S},t),\ t > 0, \tag{15}$$

and a traction condition on the elastic solid imposed by the fluid,

$$\mathbf{T}(\nabla \mathbf{y}(\mathbf{x},t),\mathbf{x})\mathbf{n}_0 = (\det \mathbf{F})\boldsymbol{\sigma}(\mathbf{y}(\mathbf{x},t),t)\mathbf{F}^{-T}\mathbf{n}_0 \quad \mathbf{x} \in \partial\Omega \setminus \mathcal{S},\ t > 0, \tag{16}$$

with $\boldsymbol{\sigma}$ defined in (11).

We could also have some additional kinematic conditions, such as anchoring conditions for the elastic body. These could be added without changing our conclusions. All of the choices in this section have the interesting property that the softer body imposes traction boundary conditions on the harder body, while the harder body imposes displacement boundary conditions on the softer body.

5 Scaling Laws

5.1 One Scaling Parameter; General Elastic Material

We take the more general point of view expressed in the introduction of seeking a change of variables such that full set of equations of motion and interaction conditions for the laboratory model implies their satisfaction for the full-scale model. Our notation going forward is to write the scaling parameters as a superscript for quantities describing the full-scale model.

The equations of motion (6) of the elastic solid are most restrictive. This is because the function $\mathbf{T}(\mathbf{F},\mathbf{x})$ is unspecified. It could be specified, by choosing for example one of the popular forms, such as Mooney-Rivlin [19], Gent-Thomas [20], or Ogden [21] materials, but these would lead to highly specialized relations among the material constants, because they

multiply different functions of $\mathbf{F}$ with apparently different powers of the scaling parameter. Few of these constants are measured. Thus, the practical problem of identifying an actual material for the laboratory model is likely to be prohibitive. There are possibilities for the one constant Neo-Hookean material, but we do not pursue this case.

The simplest possibility that avoids implication of these material constants is that the rescaling *preserves the deformation gradient*, i.e., "elasticity scaling". Ignoring the time dependence for now, this means we introduce the dimensionless scaling parameter λ and assume the deformation gradient and Piola-Kirchhoff stress for the full-scale model are

$$\mathbf{F}^{(\lambda)}(\mathbf{x},t)=\mathbf{F}(\tfrac{1}{\lambda}\mathbf{x},\tfrac{1}{\lambda}t),\quad \mathbf{T}^{(\lambda)}(\mathbf{F}^{(\lambda)}(\mathbf{x},t),\mathbf{x})=\mathbf{T}(\mathbf{F}(\tfrac{1}{\lambda}\mathbf{x},\tfrac{1}{\lambda}t),\tfrac{1}{\lambda}\mathbf{x}),\quad \mathbf{x}\in\lambda\Omega. \tag{17}$$

Our choice is to scale the inhomogeneity like the argument of $\mathbf{F}$. In view of (7) this is the right choice to make the right hand side of the equations of motion for the elastic body consistent. It also has the natural physical interpretation that inhomogeneity is simply scaled up – in the case of a layered composite the layers are simply scaled by λ, retaining their material properties within corresponding layers.

Notice that the scaling (17) brings a factor $1/\lambda$ to the right hand side of (7) due to the divergence. Elasticity scaling also implies that the elastic properties of the full-scale model are the same as the laboratory model. Here, we assume the reference densities of the model and structure are the same. To assure the equations of motion (7) for the elastic body are exactly satisfied by the full-scale model, the left hand side must satisfy

$$\rho_0^{(\lambda)}(\mathbf{x})=\rho_0(\tfrac{1}{\lambda}\mathbf{x}),\quad \mathbf{x}\in\lambda\Omega. \tag{18}$$

Satisfaction of the equations of motion of the elastic body of the full-scale model then implies

$$\mathbf{y}^{(\lambda)}(\mathbf{x},t)=\lambda\,\mathbf{y}(\tfrac{1}{\lambda}\mathbf{x},\tfrac{1}{\lambda}t), \tag{19}$$

which also implies how frequencies transform.

Since the patch $\mathcal{S}$ is shared by the elastic and rigid bodies, it must scale as the elastic body. This in turn forces elasticity scaling onto the rigid body. Thus, we must assume that the rigid body transforms by elasticity scaling, i.e.,

$$\mathbf{y}_r^{(\lambda)}(\mathbf{x},t)=\lambda\,\mathbf{y}_r(\tfrac{1}{\lambda}\mathbf{x},\tfrac{1}{\lambda}t). \tag{20}$$

Consistency of the equations of motion then forces the density of the rigid body to transform by the law

$$\rho_r^{(\lambda)}(\mathbf{x})=\rho_r(\tfrac{1}{\lambda}\mathbf{x}),\quad \mathbf{x}\in\lambda\Omega_r. \tag{21}$$

These assumptions, in turn, imply scaling laws for the total mass M_r, the center of mass $\mathbf{x}_{cm}$ and the inertia tensor $\mathcal{I}$ according to their definitions given in Sect. 3.1,

$$\begin{aligned} M_r^{(\lambda)}&=\lambda^3 M_r,\\ \mathbf{x}_{cm}^{(\lambda)}&=\lambda\mathbf{x}_{cm},\\ \mathcal{I}^{(\lambda)}&=\lambda^5\mathcal{I}, \end{aligned} \tag{22}$$

and so the motion of the rigid body for the full-scale model is

$$\mathbf{y}_r^{(\lambda)}(\mathbf{x},t)=\lambda\,\mathbf{y}_r(\tfrac{1}{\lambda}\mathbf{x},\tfrac{1}{\lambda}t)=\mathbf{R}(\tfrac{1}{\lambda}t)(\mathbf{x}-\mathbf{x}_{cm}^{(\lambda)})+\mathbf{y}_{cm}^{(\lambda)}(t). \tag{23}$$

These scaling laws are found by direct substitution of (20) into the definitions and a change of variables.

We postpone the verification of the equations of motion of the rigid body until the end of this section, because the fluid contributes to the force and moment on the rigid body.

We now turn to the scaling laws for the incompressible fluid. These must be consistent with the interaction conditions coming from the elastic solid, whose scaling has already been determined. As expressed in (15) the elastic body imposes a no slip condition on the fluid. This occurs on the deforming boundary of the elastic solid, where it meets the fluid. To understand how this restricts the motion of the fluid, it is convenient to pass to an Eulerian version of (15). We will then need to express the inverse of the motion $\mathbf{y}^{(\lambda)}(\mathbf{x},t),\ \mathbf{x}\in\lambda\Omega$, in terms of the inverse of $\mathbf{y}(\mathbf{x},t),\ \mathbf{x}\in\Omega$. We have that $\mathbf{y}^{(\lambda)}(\mathbf{x},t)=\lambda\mathbf{y}(\frac{1}{\lambda}\mathbf{x},\frac{1}{\lambda}t),\ \mathbf{x}\in\lambda\Omega$, so

$$\mathbf{x}=\mathbf{y}^{(\lambda)-1}(\mathbf{y}^{(\lambda)}(\mathbf{x},t),t)=\mathbf{y}^{(\lambda)-1}\big(\lambda\mathbf{y}(\tfrac{1}{\lambda}\mathbf{x},\tfrac{1}{\lambda}t),t\big). \tag{24}$$

Put $\mathbf{x}=\lambda\mathbf{y}^{-1}(\mathbf{r},\frac{1}{\lambda}t)$ and then put $\mathbf{r}=\lambda\mathbf{y}\in\lambda\mathbf{y}(\Omega,t)$ to get

$$\mathbf{y}^{(\lambda)-1}(\mathbf{r},t)=\lambda\mathbf{y}^{-1}\big(\tfrac{1}{\lambda}\mathbf{r},\tfrac{1}{\lambda}t\big). \tag{25}$$

Notice that the scaling of the inverse of $\mathbf{y}^{(\lambda)}(\cdot,t)$ is *the same* as the scaling of $\mathbf{y}(\mathbf{x},t)$; it is not the inverse of its scaling. Therefore, combining these results, the scaling of the Eulerian velocity field is

$$\mathbf{v}^{(\lambda)}(\mathbf{r},t)=\dot{\mathbf{y}}^{(\lambda)}\big(\mathbf{y}^{(\lambda)-1}(\mathbf{r},t),t\big)=\dot{\mathbf{y}}(\mathbf{y}^{-1}(\tfrac{1}{\lambda}\mathbf{r},\tfrac{1}{\lambda}t),\tfrac{1}{\lambda}t)=\mathbf{v}(\tfrac{1}{\lambda}\mathbf{r},\tfrac{1}{\lambda}t). \tag{26}$$

Hence, compatibility of the Navier-Stokes equation with elasticity and rigid body mechanics restricts the standard Reynold's number scaling of the Navier-Stokes equations, since space and time must be scaled alike. However, there is the useful remaining invariance (26).

Finally, consider the Navier-Stokes equations for an incompressible fluid, and suppose they are satisfied by the velocity field of the laboratory model outside the elastic and rigid bodies:

$$\mathbf{v}_t+\nabla\mathbf{v}\,\mathbf{v}=-\nabla p+\nu\Delta\mathbf{v},\quad \operatorname{div}\mathbf{v}=0,\quad \mathbf{v}(\mathbf{y},t),\ \ \mathbf{y}\in\mathbb{R}^3\setminus\big(\mathbf{y}(\Omega,t)\cup\mathbf{y}_r(\Omega_r,t)\big). \tag{27}$$

Here, as above, we have divided by the density of the fluid, so ν is kinematic viscosity and p is pressure over density. Assuming that $\mathbf{v}(\mathbf{y},t)$, $p(\mathbf{y},t)$ satisfy (27) on the given domain with kinematic viscosity ν, then

$$\mathbf{v}^{(\lambda)}(\mathbf{y},t)=\mathbf{v}(\tfrac{1}{\lambda}\mathbf{y},\tfrac{1}{\lambda}t),\quad p^{(\lambda)}(\mathbf{y},t)=p(\tfrac{1}{\lambda}\mathbf{y},\tfrac{1}{\lambda}t), \tag{28}$$

satisfy the Navier-Stokes equations on the domain $\mathbb{R}^3\setminus\big(\lambda\mathbf{y}(\Omega,t)\cup\lambda\mathbf{y}_r(\Omega_r,t)\big)$ with kinematic viscosity

$$\nu^{(\lambda)}=\lambda\nu. \tag{29}$$

Hence, scaling up ($\lambda>1$) necessitates the use of a lower kinematic viscosity fluid for the laboratory scale model.

We now check the scaling of boundary conditions. We have imposed a no slip condition (15) on the deforming boundaries between fluid and elastic solid or fluid and rigid body and, in addition, a traction condition (16). The no slip conditions for the fluid at the elastic solid and rigid body are, respectively,

$$\mathbf{v}(\mathbf{y}(\mathbf{x},t),t)=\dot{\mathbf{y}}(\mathbf{x},t),\ \ \mathbf{x}\in\partial\Omega\setminus\mathcal{S}\quad\text{and}\quad \mathbf{v}(\mathbf{y}_r(\mathbf{x},t),t)=\dot{\mathbf{y}}_r(\mathbf{x},t),\ \ \mathbf{x}\in\partial\Omega_r\setminus\mathcal{S}, \tag{30}$$

for the laboratory model. Clearly, these imply that the no slip conditions are satisfied for the full-scale model. That is, by (26), (13) and the scaling laws of $\mathbf{y}(\mathbf{x},t)$ and $\mathbf{y}_r(\mathbf{x},t)$, it follows that

$$\begin{aligned}\mathbf{v}^{(\lambda)}(\mathbf{y}^{(\lambda)}(\mathbf{x},t),t)&=\dot{\mathbf{y}}^{(\lambda)}(\mathbf{x},t),\quad \mathbf{x}\in\partial\lambda\Omega\setminus\lambda\mathcal{S}\quad\text{and}\\ \mathbf{v}^{(\lambda)}(\mathbf{y}_r^{(\lambda)}(\mathbf{x},t),t)&=\dot{\mathbf{y}}_r^{(\lambda)}(\mathbf{x},t),\quad \mathbf{x}\in\partial\lambda\Omega_r\setminus\lambda\mathcal{S}.\end{aligned}\tag{31}$$

Lastly, following (16), we consider the scaling of the traction continuity condition. For the nonlinear elastic material we have deformation gradient $\mathbf{F}(\mathbf{x},t)=\nabla\mathbf{y}(\mathbf{x},t)$, giving rise to the Cauchy stress

$$\boldsymbol{\sigma}(\mathbf{y}(\mathbf{x},t),t)=\frac{1}{\det\mathbf{F}(\mathbf{x},t)}\mathbf{T}(\mathbf{F}(\mathbf{x},t),\mathbf{x})\mathbf{F}(\mathbf{x},t)^T,\quad \mathbf{x}\in\partial\Omega\setminus\mathcal{S},\tag{32}$$

where the Cauchy stress in the Navier-Stokes fluid of density $\rho_f=const.$ is, in Eulerian form,

$$\boldsymbol{\sigma}(\mathbf{y},t)=\rho_f\big(-p(\mathbf{y},t)\mathbf{I}+2\nu\mathbf{D}(\mathbf{y},t)\big),\quad \text{where }\ \mathbf{D}=\frac{1}{2}(\nabla\mathbf{v}+(\nabla\mathbf{v})^T).\tag{33}$$

Thus, traction continuity for the laboratory model can be written as

$$\begin{aligned}&\frac{1}{\det\mathbf{F}(\mathbf{x},t)}\mathbf{T}(\mathbf{F}(\mathbf{x},t),\mathbf{x})\mathbf{F}(\mathbf{x},t)^T\mathbf{n}\\ &=\rho_f\Big(-p(\mathbf{y}(\mathbf{x},t),t)\mathbf{I}+\nu\big(\nabla\mathbf{v}(\mathbf{y}(\mathbf{x},t),t)+(\nabla\mathbf{v}(\mathbf{y}(\mathbf{x},t),t)^T\big)\Big)\mathbf{n},\quad \mathbf{x}\in\partial\Omega\setminus\mathcal{S},\end{aligned}\tag{34}$$

where $\mathbf{n}$ is the outward unit normal to $\partial\mathbf{y}(\Omega,t)\setminus\partial\mathbf{y}_r(\Omega_r,t)$. Alternatively, for computational purposes (since Ω is given) one could replace $\mathbf{n}$ in (34) by $\mathbf{F}^{-T}\mathbf{n}_0$, where $\mathbf{n}_0$ is the outward normal to $\partial\Omega\setminus\mathcal{S}$.

A similar formula as (34), integrated over $\partial\Omega_r\setminus\mathcal{S}$ holds for the rigid body. However, it does not serve as a boundary condition, but rather as a contribution to the overall force and moment that appear on the right hand side of the equations of motion of the rigid body.

We now examine the implications of (17) and (18) for traction continuity of the full-scale model. We replace $\mathbf{x},t$ in (34) by $\mathbf{x}/\lambda,t/\lambda$, use (28), (29) and $\mathbf{y}^{(\lambda)}(\mathbf{x},t)=\lambda\mathbf{y}(\frac{1}{\lambda}\mathbf{x},\frac{1}{\lambda}t)$. Also, geometric similarity (or the standard parametric formula of continuum mechanics) implies that $\mathbf{n}^{(\lambda)}=\mathbf{n}$. After making these substitutions, we obtain

$$\begin{aligned}&\frac{1}{\det\mathbf{F}^{(\lambda)}(\mathbf{x},t)}\mathbf{T}^{(\lambda)}(\mathbf{F}^{(\lambda)}(\mathbf{x},t),\mathbf{x})\mathbf{F}^{(\lambda)}(\mathbf{x},t)^T\mathbf{n}^{(\lambda)}\\ &=\rho_f\Big(-p(\mathbf{y}^{(\lambda)}(\mathbf{x},t),t)\mathbf{I}+\nu^{(\lambda)}\big(\nabla\mathbf{v}^{(\lambda)}(\mathbf{y}^{(\lambda)}(\mathbf{x},t),t)+(\nabla\mathbf{v}^{(\lambda)}(\mathbf{y}^{(\lambda)}(\mathbf{x},t),t)^T\big)\Big)\mathbf{n}^{(\lambda)}\end{aligned}\tag{35}$$

for $\mathbf{x}\in\partial\lambda\Omega\setminus\lambda\mathcal{S}$. Hence, the scaling laws (17)-(19) imply that satisfaction of traction continuity of the laboratory model (34) implies traction continuity for the full-scale model (35). See scaling laws in Table 1.

5.2 Two Scaling Parameters; Stiff Elastic Material

Notice that Piola-Kirchhoff stress as discussed in Sect. 3.2 is linear in Young's modulus. We get more options for material selection by varying the Young's modulus of the elastic solid,

and we can also allow it to be inhomogeneous. In this subsection, we introduce a scaling parameter δ for Young's modulus:

$$E^{(\lambda,\delta)}(\mathbf{x}) = \delta E(\tfrac{1}{\lambda}\mathbf{x}), \quad \mathbf{x} \in \lambda\Omega. \tag{36}$$

Assume as above $\mathbf{y}^{(\lambda)}(\mathbf{x}, t) = \lambda \mathbf{y}(\mathbf{x}/\lambda, t/\lambda)$ and that the Piola-Kirchhoff stress for the laboratory model is linear in Young's modulus having the form $E\hat{\mathbf{T}}(\mathbf{F})$. We assume that the full-scale model then has Piola-Kirchhoff stress

$$\mathbf{T}^{(\lambda,\delta)}(\mathbf{x}, t) = \delta E(\tfrac{1}{\lambda}\mathbf{x})\hat{\mathbf{T}}(\mathbf{F}(\tfrac{1}{\lambda}\mathbf{x}, \tfrac{1}{\lambda}t)), \quad \mathbf{x} \in \lambda\Omega. \tag{37}$$

The equation of motion (6) is satisfied for the full-scale model by choosing the reference density

$$\rho_0^{(\lambda,\delta)}(\mathbf{x}) = \delta\rho_0(\tfrac{1}{\lambda}\mathbf{x}), \quad \mathbf{x} \in \lambda\Omega. \tag{38}$$

Because of the choice $\mathbf{y}^{(\lambda)}(\mathbf{x}, t) = \lambda \mathbf{y}(\mathbf{x}/\lambda, t/\lambda)$, we get the same scaling for the velocity field as (26), that is,

$$\mathbf{v}^{(\lambda)}(\mathbf{r}, t) = \mathbf{v}(\tfrac{1}{\lambda}\mathbf{r}, \tfrac{1}{\lambda}t). \tag{39}$$

Assume that $\mathbf{v}(\mathbf{r}, t)$ satisfies the Navier-Stokes equations (10) on the given domain with kinematic viscosity ν. Then $\mathbf{v}^{(\lambda)}(\mathbf{y}, t) = \mathbf{v}(\frac{1}{\lambda}\mathbf{y}, \frac{1}{\lambda}t)$ satisfies the Navier-Stokes equations on the domain $\mathbb{R}^3 \setminus \big(\lambda\mathbf{y}(\Omega, t) \cup \lambda\mathbf{y}_r(\Omega_r, t)\big)$ with kinematic viscosity and pressure/density

$$\nu^{(\lambda)} = \lambda\nu, \quad p^{(\lambda)}(\mathbf{y}, t) = p(\tfrac{1}{\lambda}\mathbf{y}, \tfrac{1}{\lambda}t). \tag{40}$$

Let $\rho_f^{(\lambda,\delta)}$ denote the density of the fluid for the full-scale model. Traction continuity between elastic solid and the fluid, i.e.,

$$\begin{aligned}&\frac{1}{\det \mathbf{F}^{(\lambda)}(\mathbf{x}, t)}\mathbf{T}^{(\lambda,\delta)}(\mathbf{x}, t)\mathbf{F}^{(\lambda)}(\mathbf{x}, t)^T\mathbf{n}^{(\lambda)}\\ &= \rho_f^{(\lambda,\delta)}\big(-p^{(\lambda)}(\mathbf{y}^{(\lambda)}(\mathbf{x}, t), t)\mathbf{I} + \nu^{(\lambda)}\big(\nabla\mathbf{v}^{(\lambda)}(\mathbf{y}^{(\lambda)}(\mathbf{x}, t), t) + (\nabla\mathbf{v}^{(\lambda)}(\mathbf{y}^{(\lambda)}(\mathbf{x}, t), t)^T\big)\big)\mathbf{n}^{(\lambda)},\end{aligned} \tag{41}$$

for $\mathbf{x} \in \partial\lambda\Omega \setminus \lambda\mathcal{S}$ is then satisfied by the choice

$$\rho_f^{(\lambda,\delta)}(\mathbf{y}) = \delta\rho_f(\tfrac{1}{\lambda}\mathbf{y}) \tag{42}$$

for the full-scale model. Here, we retain the superscript λ to avoid conflict with the notation for other choices of scaling parameters, even though this dependence is trivial here due to the incompressibility of the fluid. Since the rigid body is attached to the elastic solid, the motion of the rigid body can be given as above by

$$\mathbf{y}_r^{(\lambda)}(\mathbf{x}, t) = \lambda\mathbf{y}_r(\tfrac{1}{\lambda}\mathbf{x}, \tfrac{1}{\lambda}t). \tag{43}$$

Considering the equations of motion (5) and forces (12) for the rigid body, its density will transform by the law

$$\rho_r^{(\lambda,\delta)}(\mathbf{x}) = \delta\rho_r(\tfrac{1}{\lambda}\mathbf{x}), \quad \mathbf{x} \in \lambda\Omega_r. \tag{44}$$

Then the scaling laws for the total mass M_r and the inertia tensor $\mathcal{I}$ are given for the full-scale model by

$$M_r^{(\lambda,\delta)} = \delta\lambda^3 M_r,$$
$$\mathcal{I}^{(\lambda,\delta)} = \delta\lambda^5 \mathcal{I}. \tag{45}$$

These scaling laws are summarized in Table 2.

5.3 Four Scaling Parameters; Stiff Elastic Material

In this subsection, we consider the more general case with four scaling parameters. Let λ, α, η and δ be the geometry, time, density and Young's modulus scaling parameters, respectively. Starting from elastic solid which is assumed to have Piola-Kirchhoff stress given by (9), we have

$$\mathbf{F}^{(\lambda,\alpha)}(\mathbf{x},t) = \mathbf{F}(\tfrac{1}{\lambda}\mathbf{x}, \tfrac{1}{\alpha}t),\ \ \mathbf{T}^{(\lambda,\alpha,\delta)}(\mathbf{x},t) = \delta E(\tfrac{1}{\lambda}\mathbf{x})\hat{\mathbf{T}}(\mathbf{F}(\tfrac{1}{\lambda}\mathbf{x}, \tfrac{1}{\alpha}t)), \tag{46}$$

$$\rho_0^{(\eta,\lambda)}(\mathbf{x}) = \eta\rho_0(\tfrac{1}{\lambda}\mathbf{x}),\ \ \mathbf{y}^{(\lambda,\alpha)}(\mathbf{x},t) = \lambda\mathbf{y}(\tfrac{1}{\lambda}\mathbf{x}, \tfrac{1}{\alpha}t), \quad \mathbf{x} \in \lambda\Omega. \tag{47}$$

Then (6) is satisfied for the full-scale structure if and only if the four parameters satisfy

$$\eta = \delta\frac{\alpha^2}{\lambda^2}. \tag{48}$$

For the fluid, since $\mathbf{y}^{(\lambda,\alpha)}(\mathbf{x},t) = \lambda\mathbf{y}(\frac{1}{\lambda}\mathbf{x}, \frac{1}{\alpha}t)$, we get

$$\mathbf{v}^{(\lambda,\alpha)}(\mathbf{r},t) = \dot{\mathbf{y}}^{(\lambda,\alpha)}\big(\mathbf{y}^{(\lambda,\alpha)-1}(\mathbf{r},t),t\big) = \lambda\dot{\mathbf{y}}(\mathbf{y}^{-1}(\tfrac{1}{\lambda}\mathbf{r}, \tfrac{1}{\alpha}t), \tfrac{1}{\alpha}t) = \tfrac{\lambda}{\alpha}\mathbf{v}(\tfrac{1}{\lambda}\mathbf{r}, \tfrac{1}{\alpha}t). \tag{49}$$

Consider the Navier-Stokes equations for an incompressible fluid, and assume that $\mathbf{v}(\mathbf{y},t)$ satisfies (10) on the given domain with kinematic viscosity ν. Then (49) satisfies the Navier-Stokes equations on the domain $\mathbb{R}^3 \setminus \big(\lambda\mathbf{y}(\Omega,t) \cup \lambda\mathbf{y}_r(\Omega_r,t)\big)$ with kinematic viscosity and pressure

$$\nu^{(\lambda,\alpha)} = \tfrac{\lambda^2}{\alpha}\nu, \quad p^{(\lambda,\alpha)}(\mathbf{y},t) = \tfrac{\lambda^2}{\alpha^2}p(\tfrac{1}{\lambda}\mathbf{y}, \tfrac{1}{\alpha}t). \tag{50}$$

Then considering traction continuity between elastic solid and the fluid, we have

$$\begin{aligned}
&\frac{1}{\det\mathbf{F}^{(\lambda,\alpha)}(\mathbf{x},t)}\mathbf{T}^{(\lambda,\alpha,\delta)}(\mathbf{x},t)\mathbf{F}^{(\lambda,\alpha)}(\mathbf{x},t)^T\mathbf{n}^{(\lambda)} \\
&= -\rho_f^{(\lambda,\alpha,\delta)}p^{(\lambda,\alpha)}(\mathbf{y}^{(\lambda,\alpha)}(\mathbf{x},t),t)\mathbf{n}^{(\lambda)} \\
&\quad + \rho_f^{(\lambda,\alpha,\delta)}\nu^{(\lambda,\alpha)}\big(\nabla\mathbf{v}^{(\lambda,\alpha)}(\mathbf{y}^{(\lambda,\alpha)}(\mathbf{x},t),t) + (\nabla\mathbf{v}^{(\lambda,\alpha)}(\mathbf{y}^{(\lambda,\alpha)}(\mathbf{x},t),t)^T\big)\mathbf{n}^{(\lambda)},
\end{aligned} \tag{51}$$

for $\mathbf{x} \in \partial\lambda\Omega \setminus \lambda\mathcal{S}$. Substituting all quantities to (51), we get

$$\rho_f^{(\lambda,\alpha,\delta)}(\mathbf{y}) = \delta\tfrac{\alpha^2}{\lambda^2}\rho_f(\tfrac{1}{\lambda}\mathbf{y}). \tag{52}$$

Again, we retain the superscript λ to avoid conflict with the notation for other choices of scaling parameters, even though this dependence is trivial here due to the incompressibility of the fluid. The motion of the rigid body is restricted by the motion of elastic solid, yielding

$$\mathbf{y}_r^{(\lambda,\alpha)} = \lambda\mathbf{y}_r(\tfrac{1}{\lambda}\mathbf{x}, \tfrac{1}{\alpha}t). \tag{53}$$

Similarly, consistency with (5) and (12) implies that the scaling law for density of rigid body is

$$\rho_r^{(\lambda,\alpha,\delta)}(\mathbf{x}) = \delta\frac{\alpha^2}{\lambda^2}\rho_r(\tfrac{1}{\lambda}\mathbf{x}), \quad \mathbf{x} \in \lambda\Omega_r. \tag{54}$$

Correspondingly, the total mass M_r and the inertia tensor $\mathcal{I}$ of rigid bodies will transfer by

$$\begin{aligned} M_r^{(\lambda,\alpha,\delta)} &= \delta\alpha^2\lambda M_r, \\ \mathcal{I}^{(\lambda,\alpha,\delta)} &= \delta\alpha^2\lambda^3\mathcal{I}. \end{aligned} \tag{55}$$

The scaling laws in this case are summarized in Table 3.

6 Summary of Scalings

Summaries of the scaling laws are given in Tables 1, 2 and 3.

Remarks and Examples for Table 1 In this case, since the density and elastic properties of the corresponding solid structures in the two models are the same, one can simply choose the materials used to make the full-scale structure to fabricate the corresponding laboratory structure at scale. Note that the fluids in the two models are different since they have same density but different kinematic viscosity. We can choose fluids with lower kinematic viscosity but similar density as the full-scale fluid. Another way to design such fluids for the laboratory model is to choose the same fluid as full-scale model to guarantee the same density, then varying the temperature of a closed tunnel to obtain lower kinematic viscosity and therefore higher geometric scaling parameter λ.

Remarks and Examples for Table 2 The scaling of Young's modulus opens up more possibilities for material selection. For our motivating example of a Vertical Axis Wind Turbine (VAWT), assume the full-scale structure has the rotor diameter of approximately $1m$, and the blades are made of fiberglass reinforced polyester with $\rho \approx 1600\,\mathrm{kg/m^3}$ and $E \approx 20\,\mathrm{GPa}$. At room temperature and atmospheric pressure, the full-scale fluid has $\nu_{air} = 15.6 \times 10^{-6}\,\mathrm{m^2/s}$

Table 1 Scaling laws with one geometric scaling parameter (λ) and a general elastic material

Variable	Rigid body		Elastic solid		Fluid	
	Laboratory	Full-scale	Laboratory	Full-scale	Laboratory	Full-scale
Geometry	$\mathbf{x} \in \Omega_r$	$\mathbf{x} \in \lambda\Omega_r$	$\mathbf{x} \in \Omega$	$\mathbf{x} \in \lambda\Omega$		
Time	$t \in T$	$t \in \lambda T$	$t \in T$	$t \in \lambda T$	$t \in T$	$t \in \lambda T$
Density	$\rho_r(\mathbf{x})$	$\rho_r(\frac{1}{\lambda}\mathbf{x})$	$\rho_0(\mathbf{x})$	$\rho_0(\frac{1}{\lambda}\mathbf{x})$	$\rho_f(\mathbf{r})$	$\rho_f(\frac{1}{\lambda}\mathbf{r})$
Mass	M_r	$\lambda^3 M_r$	M	$\lambda^3 M$		
Young's modulus			E	E		
Motion	$\mathbf{y}_r(\mathbf{x}, t)$	$\lambda\,\mathbf{y}_r(\frac{1}{\lambda}\mathbf{x}, \frac{1}{\lambda}t)$	$\mathbf{y}(\mathbf{x}, t)$	$\lambda\,\mathbf{y}(\frac{1}{\lambda}\mathbf{x}, \frac{1}{\lambda}t)$	$\mathbf{v}(\mathbf{r}, t)$	$\mathbf{v}(\frac{1}{\lambda}\mathbf{r}, \frac{1}{\lambda}t)$
Deformation gradient	$\mathbf{R}(t)$	$\mathbf{R}(\frac{1}{\lambda}t)$	$\mathbf{F}(\mathbf{x}, t)$	$\mathbf{F}(\frac{1}{\lambda}\mathbf{x}, \frac{1}{\lambda}t)$		
Kinematic viscosity					ν	$\lambda\nu$
Pressure/density					$p(\mathbf{r}, t)$	$p(\frac{1}{\lambda}\mathbf{r}, \frac{1}{\lambda}t)$
Cauchy Stress			$\boldsymbol{\sigma}(\mathbf{x}, t)$	$\boldsymbol{\sigma}(\frac{1}{\lambda}\mathbf{x}, \frac{1}{\lambda}t)$	$\boldsymbol{\sigma}_f(\mathbf{r}, t)$	$\boldsymbol{\sigma}_f(\frac{1}{\lambda}\mathbf{r}, \frac{1}{\lambda}t)$

Table 2 Scaling laws with scaling parameters for geometry (λ) and Young's modulus (δ) (stiff elastic material)

Variable	Rigid body		Elastic solid		Fluid	
	Laboratory	Full-scale	Laboratory	Full-scale	Laboratory	Full-scale
Geometry	$\mathbf{x} \in \Omega_r$	$\mathbf{x} \in \lambda\Omega_r$	$\mathbf{x} \in \Omega$	$\mathbf{x} \in \lambda\Omega$		
Time	$t \in T$	$t \in \lambda T$	$t \in T$	$t \in \lambda T$	$t \in T$	$t \in \lambda T$
Density	$\rho_r(\mathbf{x})$	$\delta\rho_r(\frac{1}{\lambda}\mathbf{x})$	$\rho_0(\mathbf{x})$	$\delta\rho_0(\frac{1}{\lambda}\mathbf{x})$	$\rho_f(\mathbf{r})$	$\delta\rho_f(\frac{1}{\lambda}\mathbf{r})$
Mass	M_r	$\delta\lambda^3 M_r$	M	$\delta\lambda^3 M$		
Young's modulus			E	δE		
Motion	$\mathbf{y}_r(\mathbf{x}, t)$	$\lambda\,\mathbf{y}_r(\frac{1}{\lambda}\mathbf{x}, \frac{1}{\lambda}t)$	$\mathbf{y}(\mathbf{x}, t)$	$\lambda\,\mathbf{y}(\frac{1}{\lambda}\mathbf{x}, \frac{1}{\lambda}t)$	$\mathbf{v}(\mathbf{r}, t)$	$\mathbf{v}(\frac{1}{\lambda}\mathbf{r}, \frac{1}{\lambda}t)$
Deformation gradient	$\mathbf{R}(t)$	$\mathbf{R}(\frac{1}{\lambda}t)$	$\mathbf{F}(\mathbf{x}, t)$	$\mathbf{F}(\frac{1}{\lambda}\mathbf{x}, \frac{1}{\lambda}t)$		
Kinematic viscosity					ν	$\lambda\nu$
Pressure/density					$p(\mathbf{r}, t)$	$p(\frac{1}{\lambda}\mathbf{r}, \frac{1}{\lambda}t)$
Cauchy Stress			$\boldsymbol{\sigma}(\mathbf{x}, t)$	$\delta\boldsymbol{\sigma}(\frac{1}{\lambda}\mathbf{x}, \frac{1}{\lambda}t)$	$\boldsymbol{\sigma}_f(\mathbf{r}, t)$	$\delta\boldsymbol{\sigma}_f(\frac{1}{\lambda}\mathbf{r}, \frac{1}{\lambda}t)$

and $\rho_{air} = 1.204\ \mathrm{kg/m^3}$. One way to design the laboratory fluid is to use pressurized air [22]. For example, at room temperature and 6 times atmospheric pressure, the kinematic viscosity and density of air become $\bar{\nu}_{air} = 2.603 \times 10^{-6}\ \mathrm{m^2/s}$ and $\bar{\rho}_{air} = 7.122\ \mathrm{kg/m^3}$, giving scaling parameters $\lambda \approx 6$ and $\delta \approx 1/6$. According to Table 2, this implies (1) the size of laboratory VAWT will be reduced to 1/6 of the full-scale VAWT (to approx. 17 cm); (2) both density and Young's modulus of the laboratory blades will increase to 6 times that of the full-scale blades, which are approximately 9600 $\mathrm{kg/m^3}$ and 120 GPa. We can select suitable metals or alloys to fabricate the laboratory blades, see the plot of Young's modulus against density in page 61 of [23]. Particularly, copper with density $\approx 9000\ \mathrm{kg/m^3}$ and Young's modulus ≈ 120 GPa would be an option.

Modern thermoplastic resins used in many industries, such as horizontal axis wind turbines and automobiles, have $E \approx 2$ GPa and $\rho \approx 1000\ \mathrm{kg/m^3}$, giving a wide variety of possible scale factors with metals or hard polymers chosen for the laboratory model. If we increase pressure to 11 times atmospheric pressure, at room temperature, we have $\bar{\nu}_{air} = 1.42 \times 10^{-6}\ \mathrm{m^2/s}$ and $\bar{\rho}_{air} = 13.08\ \mathrm{kg/m^3}$, then the scaling parameters will be $\lambda \approx 11$ and $\delta \approx \frac{1}{11}$. So for the laboratory structure, we get (1) size reduction to 1/11 of the size of full-scale structure; (2) density: $\rho/\delta \approx 11000\ \mathrm{kg/m^3}$, and (3) Young's modulus: $E/\delta \approx 22$ GPa. Therefore, lead alloys with density $\approx 11000\ \mathrm{kg/m^3}$ and Young's modulus ≈ 21 GPa will be a possible option to fabricate the laboratory structure.

Timber has been the main building material for house construction, especially in earthquake-prone areas. One can use above method to design laboratory model to test the structural stability. Specially, if the geometric scaling parameter is chosen as $\lambda = 20$, low carbon steel will be a suitable material to fabricate laboratory model, and the test environment will be 20 times atmospheric pressure.

Remarks and Examples for Table 3 In this general case, one more independent scaling parameter, α for time, is introduced, which gives us additional flexibility to design the scale model. Reduction of the duration of the experiment can be achieved by increasing the value of α.

In addition, since we have $\eta = \delta\frac{\alpha^2}{\lambda^2}$, the inverse design of densities of laboratory fluid can be realized by adjusting the three independent parameters on the right-hand side. For example, if we choose the laboratory fluid same as the full-scale fluid, the scaling parameters

Table 3 Scaling laws with the scaling of geometry (λ), time (α), density (η) and Young's modulus (δ), where $\eta = \delta\alpha^2/\lambda^2$ (stiff elastic material)

Variable	Rigid body		Elastic solid		Fluid	
	Laboratory	Full-scale	Laboratory	Full-scale	Laboratory	Full-scale
Geometry	$\mathbf{x} \in \Omega_r$	$\mathbf{x} \in \lambda\Omega_r$	$\mathbf{x} \in \Omega$	$\mathbf{x} \in \lambda\Omega$		
Time	$t \in T$	$t \in \alpha T$	$t \in T$	$t \in \alpha T$	$t \in T$	$t \in \alpha T$
Density	$\rho_r(\mathbf{x})$	$\frac{\delta\alpha^2}{\lambda^2}\rho_r(\frac{1}{\lambda}\mathbf{x})$	$\rho_0(\mathbf{x})$	$\frac{\delta\alpha^2}{\lambda^2}\rho_0(\frac{1}{\lambda}\mathbf{x})$	$\rho_f(\mathbf{r})$	$\frac{\delta\alpha^2}{\lambda^2}\rho_f(\frac{1}{\lambda}\mathbf{r})$
Mass	M_r	$\delta\alpha^2\lambda M_r$	M	$\delta\alpha^2\lambda M$		
Young's modulus			E	δE		
Motion	$\mathbf{y}_r(\mathbf{x}, t)$	$\lambda\,\mathbf{y}_r(\frac{1}{\lambda}\mathbf{x}, \frac{1}{\alpha}t)$	$\mathbf{y}(\mathbf{x}, t)$	$\lambda\,\mathbf{y}(\frac{1}{\lambda}\mathbf{x}, \frac{1}{\alpha}t)$	$\mathbf{v}(\mathbf{r}, t)$	$\frac{\lambda}{\alpha}\mathbf{v}(\frac{1}{\lambda}\mathbf{r}, \frac{1}{\alpha}t)$
Deformation gradient	$\mathbf{R}(t)$	$\mathbf{R}(\frac{1}{\alpha}t)$	$\mathbf{F}(\mathbf{x}, t)$	$\mathbf{F}(\frac{1}{\lambda}\mathbf{x}, \frac{1}{\alpha}t)$		
Kinematic viscosity					ν	$\frac{\lambda^2}{\alpha}\nu$
Pressure/density					$p(\mathbf{r}, t)$	$\frac{\lambda^2}{\alpha^2}p(\frac{1}{\lambda}\mathbf{r}, \frac{1}{\alpha}t)$
Cauchy Stress			$\boldsymbol{\sigma}(\mathbf{x}, t)$	$\delta\boldsymbol{\sigma}(\frac{1}{\lambda}\mathbf{x}, \frac{1}{\lambda}t)$	$\boldsymbol{\sigma}_f(\mathbf{r}, t)$	$\delta\boldsymbol{\sigma}_f(\frac{1}{\lambda}\mathbf{r}, \frac{1}{\alpha}t)$

will satisfy $\eta = \delta\frac{\alpha^2}{\lambda^2} = 1$ and $\frac{\lambda^2}{\alpha} = 1$. Assume the size of laboratory structure is reduced to $1/10$ of the full-scale structure, i.e., $\lambda = 10$, we get $\alpha = 100$ and $\delta = \frac{1}{100}$. Therefore, the laboratory structure has approximately 100 times Young's modulus but similar density of the full-scale structure. Ethylene tetrafluoroethylene (ETFE) has been a widely used building material in aerospace industry, agricultural and architectural projects, such as the panels to cover the outside of the football stadium Allianz Arena or the Beijing National Aquatics Centre and ETFE roof at Manchester Piccadilly station in UK. Model experiments will play a guiding role in the construction of such architectures. For the full-scale structure we have $E \approx 0.85$ GPa and $\rho \approx 1680\ \mathrm{kg/m^3}$ for ETFE. Then carbon fiber reinforced polyester (CFRP) with E of $70GPa - 150$ GPa and $\rho \approx 1.6\ \mathrm{g/cm^3}$ will be a suitable material to build the laboratory structure with scaling parameters $\lambda = 10$, $\eta \approx 1$ and $\delta \approx \frac{1}{100}$.

These scaling laws can be used not only to design size-reduced laboratory models for large-scale structures but also to design size-increased laboratory models for small-scale structures. An interesting example is the study of the role of elastic effects in biomimetic shark skin. Shark skin surface with its unique microstructure can achieve flow-drag reduction [24, 25]. A scaled-up model satisfying dynamic similarity would be helpful to understand the underlying mechanism, which can then be applied to design structures with better drag reduction performance. The full-scale shark skin has $E \approx 0.2$ GPa and $\rho \approx 800\ \mathrm{kg/m^3}$. For the laboratory model, we scale up the microstructure 15 times, i.e., $\lambda = \frac{1}{15}$, and let laboratory fluid be water, we get $\eta = 1$ and $\delta = 225$. Then rubber with $E \approx 0.9$ MPa and $\rho \approx 800\ \mathrm{kg/m^3}$, such as silicone, acrylic rubber, chlorinated polyethylene rubber, etc., would be suitable materials. Of course, Reynolds numbers of the two models are necessarily the same. In this analysis we have assumed that the elasticity of shark skin is reasonably modeled by a geometrically nonlinear – physically linear model, which would have to be tested.

7 The Full System of Equations

As a basis for studies of well-posedness, we give a statement of the full system of equations for the laboratory model to clarify all the couplings.

1. Equations of motion of the nonlinear elastic body

$$\rho_0(\mathbf{x})\ddot{\mathbf{y}} = \mathrm{div}_{\mathbf{x}}\mathbf{T}, \quad \mathbf{x} \in \Omega, \quad t > 0. \tag{56}$$

This is to be solved for $\mathbf{y}(\mathbf{x}, t),\ \mathbf{x} \in \Omega$. The reference density $\rho_0(\mathbf{x})$ is given on Ω.

(a) Boundary conditions for the elastic body interacting with the fluid

$$\boldsymbol{\sigma}(\mathbf{x}, t)\mathbf{n} = \rho_f\Big(- p(\mathbf{y}(\mathbf{x}, t), t)\mathbf{I} + \nu\big(\nabla\mathbf{v}(\mathbf{y}(\mathbf{x}, t), t) + (\nabla\mathbf{v}(\mathbf{y}(\mathbf{x}, t), t)^T\big)\Big)\mathbf{n},$$
$$\mathbf{x} \in \partial\Omega \setminus \mathcal{S}, \tag{57}$$

where $\boldsymbol{\sigma} = \frac{1}{\det\mathbf{F}}\mathbf{T}\mathbf{F}^T$, $\mathbf{F} = \nabla_{\mathbf{x}}\mathbf{y}$.

(b) Boundary conditions for the elastic body interacting with the rigid body

$$\mathbf{y}(\mathbf{x}, t) = \mathbf{y}_r(\mathbf{x}, t) = \mathbf{R}(t)(\mathbf{x} - \mathbf{x}_{cm}) + \mathbf{y}_{cm}(t),\ \mathbf{x} \in \mathcal{S} = \partial\Omega \cap \partial\Omega_r, \tag{58}$$

2. Equations of motion of the rigid body

$$\begin{aligned} M_r\ddot{\mathbf{y}}_{cm}(t) &= \mathbf{f}(t), \\ \mathcal{I}\dot{\mathbf{w}} &= -\mathbf{w} \times \mathcal{I}\mathbf{w} - \mathbf{R}(t)^T\big(\mathbf{y}_{cm}(t) \times \mathbf{f}(t)\big) + \mathbf{m}(t), \\ \dot{\mathbf{R}} &= \mathbf{R}\mathbf{W}, \quad \mathbf{w} = \mathrm{axl}(\mathbf{W}), \quad (\text{in RCC},\ W_{ik} = \varepsilon_{ijk}w_j) \end{aligned} \tag{59}$$

where

$$\begin{aligned} M_r &= \int_{\Omega_r} \rho_0(\mathbf{x})\, d\mathbf{x} \\ \mathbf{x}_{cm} &= \frac{1}{M_r}\int_{\Omega_r} \mathbf{x}\,\rho_0(\mathbf{x})\, d\mathbf{x} \\ \mathcal{I} &= \int_{\Omega_r} \rho_0(\mathbf{x})\big[|\mathbf{x} - \mathbf{x}_{cm}|^2\mathbf{I} - (\mathbf{x} - \mathbf{x}_{cm}) \otimes (\mathbf{x} - \mathbf{x}_{cm})\big]d\mathbf{x}. \end{aligned} \tag{60}$$

(a) Forces and moments on the rigid body due to the fluid and elastic solid.
Let

$$\boldsymbol{\sigma}_f(\mathbf{x}, t) = \rho_f\Big(- p(\mathbf{y}_r(\mathbf{x}, t), t)\mathbf{I} + \nu\big(\nabla\mathbf{v}(\mathbf{y}_r(\mathbf{x}, t), t) + (\nabla\mathbf{v}(\mathbf{y}_r(\mathbf{x}, t), t)^T\big)\Big), \tag{61}$$

be the Cauchy stress in the fluid at the boundary with the rigid body, expressed in Lagrangian variables. Then, the force and moment on the rigid body from the fluid and elastic solid are,

$$\begin{aligned} \mathbf{f}(t) &= \int_{\partial\Omega_r\setminus\mathcal{S}} \boldsymbol{\sigma}_f(\mathbf{x}, t)\mathbf{R}\mathbf{n}_0\, da_0 + \int_{\mathcal{S}} \mathbf{T}\mathbf{n}_0\, da_0, \\ \mathbf{m}(t) &= \int_{\partial\Omega_r\setminus\mathcal{S}} \mathbf{y}_r(\mathbf{x}, t) \times \boldsymbol{\sigma}_f(\mathbf{x}, t)\mathbf{R}\mathbf{n}_0\, da_0 + \int_{\mathcal{S}} \mathbf{y}_0 \times \mathbf{T}\mathbf{n}_0\, da_0. \end{aligned} \tag{62}$$

In these two formulae $\mathbf{n}_0$ is the *outward normal of* Ω_r, and $\mathbf{T}$ is the Piola-Kirchhoff stress evaluated from the nonlinear elastic solution. The $\mathbf{R}$ occurs from the conversion

to Piola-Kirchhoff stress. These forms are preferable to other formulations because there are no inversions and the domain of integration is fixed.

3. Equations of motion of the Navier-Stokes fluid

$$\mathbf{v}_t + \nabla \mathbf{v}\,\mathbf{v} = -\nabla p + \nu \Delta \mathbf{v}, \quad \operatorname{div} \mathbf{v} = 0, \quad \mathbf{y} \in \mathbb{R}^3 \setminus \big(\mathbf{y}(\Omega, t) \cup \mathbf{y}_r(\Omega_r, t)\big), \tag{63}$$

to be solved for $p(\mathbf{y}, t)$ and $\mathbf{v}(\mathbf{y}, t)$.

(a) No slip condition for the fluid.

The no slip conditions for the fluid on the solid and rigid body are:

$$\mathbf{v}(\mathbf{y}(\mathbf{x}, t), t) = \dot{\mathbf{y}}(\mathbf{x}, t), \quad \mathbf{x} \in \partial\Omega \setminus \mathcal{S} \quad \text{and} \quad \mathbf{v}(\mathbf{y}_r(\mathbf{x}, t), t) = \dot{\mathbf{y}}_r(\mathbf{x}, t), \quad \mathbf{x} \in \partial\Omega_r \setminus \mathcal{S}. \tag{64}$$

(b) Conditions at infinity for the fluid, such as

$$\mathbf{v}(\mathbf{r}, t) \to \mathbf{v}_0, \ \boldsymbol{\sigma}_f(\mathbf{r}, t) = -\rho_f p(\mathbf{r}, t)\mathbf{I}, \quad \text{as } |\mathbf{r}| \to \infty. \tag{65}$$

8 Conclusion and Outlook

We have derived scaling laws for a interacting system of rigid bodies, elastic bodies and incompressible fluids undergoing large motions (geometrically nonlinear case). Our method is to investigate rescalings that preserve the equations of motion and interaction conditions between bodies. A number of cases of practical importance emerge from this analysis that to our knowledge have not been identified, and we give particular examples in Sect. 6.

For a full treatment, our motivating example of a vertical axis wind turbine would have to include a torque arising from induction in the generator, as well as possible sources of friction, tuned appropriately for the laboratory model. Apparently, this is straightforward for sufficiently simple models of induction and friction.

The classic application of dynamical similarity is to the case of large bodies scaled down to laboratory size. But the opposite case is also of modern interest, particularly for biological problems and medical devices having components with sizes from microscale to millimeter scale, where continuum theories are often accurate and the geometrically nonlinear case is required. With swimming bacteria, flying insects or biological motors, thermodynamics and chemical reactions would need to be included. It would be interesting to know if there is a theory of dynamical similarity involving scale-up to laboratory size in some of these cases.

Acknowledgements The research at UMN was supported by the MURI program (FA9550-18-1-0095 and FA9550-16-1-0566) and a Vannevar Bush Faculty Fellowship. P.B. and K.S. were supported by the LUCI project, "Phase Transition-Assisted Optimization in Bifurcated Design Spaces".

Author contributions The need for an analysis of dynamical similarity in this generality arose from research of H.L. Co-authors K.J., V.S., A.K., K.S. and P.Y. contributed to this work in part by successfully solving the problem on "Continuum Mechanics" of the Written Preliminary Exam for the AEM department. R.D.J. wrote the first draft with input from H.L. and K.J.

Declarations

Competing interests The authors declare no competing interests.

References

1. Little Heath, T., et al.: The Works of Archimedes. Courier Corporation, Chelmsford (2002)
2. Timoshenko, S.: History of Strength of Materials: With a Brief Account of the History of Theory of Elasticity and Theory of Structures. Courier Corporation, Chelmsford (1983)
3. Euler, L.: Scientia naualis seu tractatus de construendis ac dirigendis pars prior [-pars posterior] complectens theoriam vniuersam de situ ac motu corporum aquae innatantium. Typis Academiae Scientiarum, vol. 2 (1749)
4. Euler, L.: Opera Omnia vol. 18. Birkhäuser, Bäsel (1967)
5. Euler, L.: Opera Omnia vol. 19. Birkhäuser, Bäsel (1972)
6. Coutinho, C.P., Baptista, A.J., Rodrigues, J.D.: Reduced scale models based on similitude theory: a review up to 2015. Eng. Struct. **119**, 81–94 (2016)
7. Kline, S.J.: Similitude and Approximation Theory. Springer, Berlin (2012)
8. Casaburo, A., Petrone, G., Franco, F., De Rosa, S.: A review of similitude methods for structural engineering. Appl. Mech. Rev. **71**(3), 030802 (2019)
9. Birkhoff, G.: Hydrodynamics. Princeton University Press, Princeton (1960)
10. Truesdell, C., Noll, W.: The Non-linear Field Theories of Mechanics. Springer, Berlin (2004)
11. Olver, P.J.: Applications of Lie Groups to Differential Equations, vol. 107. Springer, Berlin (1993)
12. Choma, J.: In: Morphing: A Guide to Mathematical Transformations for Architects, Designers, Hachette, UK (2015)
13. Liu, H., Plucinsky, P., Feng, F., Soor, A., James, R.D.: Origami and the structure of materials. SIAM News **55**(01) (2022)
14. Velvaluri, P., Soor, A., Plucinsky, P., Lima de Miranda, R., James, R.D., Quandt, E.: Origami-inspired thin-film shape memory alloy devices. Sci. Rep. **11**(1), 1–10 (2021)
15. Dafermos, C.M.: Hyperbolic Conservation Laws in Continuum Physics. Springer, Berlin (2016)
16. Coleman, B.D., Noll, W.: The thermodynamics of elastic materials with heat conduction and viscosity. In: The Foundations of Mechanics and Thermodynamics, pp. 145–156. Springer, Berlin (1974)
17. Raoult, A.: Non-polyconvexity of the stored energy function of a Saint Venant-Kirchhoff material. Apl. Mat. **31**(6), 417–419 (1986)
18. Friesecke, G., James, R.D., Müller, S.: A theorem on geometric rigidity and the derivation of nonlinear plate theory from three-dimensional elasticity. Commun. Pure Appl. Math. **55**(11), 1461–1506 (2002)
19. Mooney, M.: A theory of large elastic deformation. J. Appl. Phys. **11**(9), 582–592 (1940)
20. Gent, A.N., Thomas, A.G.: Forms for the stored (strain) energy function for vulcanized rubber. J. Polym. Sci. **28**(118), 625–628 (1958)
21. Ogden, R.W.: Large deformation isotropic elasticity–on the correlation of theory and experiment for incompressible rubberlike solids. Proc. R. Soc. Lond. Ser. A, Math. Phys. Sci. **326**(1567), 565–584 (1972)
22. Miller, M.A., Kiefer, J., Westergaard, C., Hansen, M.O.L., Hultmark, M.: Horizontal axis wind turbine testing at high Reynolds numbers. Phys. Rev. Fluids **4**(11), 110504 (2019)
23. Ashby, M.F.: Materials Selection in Mechanical Design. Elsevier, Amsterdam (2011)
24. Dean, B., Bhushan, B.: Shark-skin surfaces for fluid-drag reduction in turbulent flow: a review. Philos. Trans. - Royal Soc., Math. Phys. Eng. Sci. **368**(1929), 4775–4806 (2010)
25. Wen, L., Weaver, J.C., Lauder, G.V.: Biomimetic shark skin: design, fabrication and hydrodynamic function. J. Exp. Biol. **217**(10), 1656–1666 (2014)

Publisher's Note Springer Nature remains neutral with regard to jurisdictional claims in published maps and institutional affiliations.

Springer Nature or its licensor (e.g. a society or other partner) holds exclusive rights to this article under a publishing agreement with the author(s) or other rightsholder(s); author self-archiving of the accepted manuscript version of this article is solely governed by the terms of such publishing agreement and applicable law.